

ADDIS ABABA UNIVERSITY
SCHOOL OF GRADUATE STUDIES

**COMPARISON OF POTENTIOMETRIC SENSORS WITH
AMPEROMETRIC SENSORS FOR DETERMINATION OF NITRATE**

Solomon Mehretie

June, 1999

COMPARISON OF POTENTIOMETRIC SENSORS WITH AMPEROMETRIC
SENSORS FOR DETERMINATION OF NITRATE

A Thesis Presented to the
School of Graduate Studies
Addis Ababa University

In Partial Fulfilment of the
Requirements for the Degree of
Master of Science in Chemistry

Solomon Mehretie

June, 1999

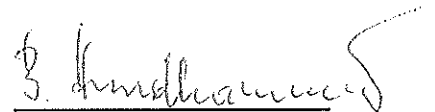
ADDIS ABABA UNIVERSITY
SCHOOL OF GRADUATE STUDIES

Comparison of Potentiometric Sensors
with Amperometric Sensors for
Determination of Nitrate

Solomon Mehretie
Chemistry Department
Faculty of Science

Approved by:

Dr. B. Hundhammer
Advisor



Dr. B.S. Chandravanshi
Examiner



Prof. Theodros Solomon
Examiner



TO MY PARENTS

ACKNOWLEDGMENT

I am greatly indebted to my advisor, Dr. Bernd Hundhammer for his generous advise, devoted assistance, encouragement in all stages of the work, constant guidance and constructive criticism which were necessary for the progress of the research.

I would like to express my thanks to all my instructors in the Department of Chemistry, above all Dr. B.S. Chandravanshi and Dr. Wendimagegn Mammo for their encouragement and valuable comments.

I am grateful Ato Nugessie Megersa for his cooperation at all times of the research. My thanks also go to Abebaw Gedefaw and Tesfaye Hailu for their valuable discussions and friendship.

I am also grateful to all my friends for their encouragement, and Azeb Yigezu for her cooperation at all times of the work.

The German Academic Exchange Service (Deutscher Akademischer Austauschdienst /DAAD) is acknowledged for giving me in-country scholarship during the M. Sc. Program. The Swedish Agency for Research Cooperation with Developing Countries (SAREC) is also acknowledged for the financial assistance.

CONTENTS

Acknowledgment	i
Contents	ii
List of Figures	iv
List of Tables	vi
Abstract	vii
1. INTRODUCTION	1
2. THEORY	6
2.1. Potentiometric Responses of Liquid State ISEs	6
2.2. Theory of the Sensor Response	8
2.3. Amperometric Response of the Sensor	10
2.4. Flow Injection Analysis	11
2.5. UV- Visible Absorption	12
3. EXPERIMENTAL	13
3.1. A Modified four Electrode Potentiostat with iR Compensation	16
4. RESULTS AND DISCUSSION	18
4.1. Response Behavior of the Potentiometric Sensor	18
4.2. Response Behavior of Amperometric Sensor	22
4.3. Dependence of Peak Potential on the Flow Rate	28

LIST OF FIGURES

1. Schematic diagram of a membrane-stabilized interface.	8
2. a) Block diagram of the flow injection system.	
b) Schematic diagram of the wall-jet cell.	14
3. Diagram of amperometric cell.	15
4. Electronic circuit of the four electrode potentiostat.	17
5. Response behavior of the potentiometric sensor at different concentrations of PNPNO_3 .	19
6. Response of the potentiometric sensor under flow and stationary conditions.	21
7. Calculated concentration change at a membrane stabilized interface of a liquid state ISE under flow conditions.	23
8. Dependence of the peak current on the applied potential difference.	25
9. Calibration graph of nitrate ion transfer at $E = 0 \text{ V}$ under flow system.	26
10. Instrument response for zero analyte concentration under flow system.	27
11. Dependence of FI-peak potential for nitrate ion on the flow rate.	28
12. Dependence of the FI-peak for nitrate transfer on the flow rate.	29

13. Potentiometric recorder protocol of the FI system.	31
14. Response of potentiometric sensor to chloride for different constant concentrations of KCl.	33
15. Response of the nitrate sensor to perchlorate ions.	35
16. Calculated response of a nitrate ISE to interfering ions Cl^- , I^- and ClO_4^- .	37
17. Experimental response of nitrate sensor to the interfering ions, Cl^- and ClO_4^- under flow condition.	37
18. Standard addition plot of potentiometric sensor.	39
19. Standard addition plot of amperometric sensor.	39
20. Recorder protocol of the UV-detector with nitrate.	41
21. a) Recorder protocol of the standard addition of the UV-detector with nitrate.	
b) Standard addition plot.	42

LIST OF TABLES

1. The influence of amount of PNPNO ₃ in the organic phase on the performance of the sensor.	18
2. The performance of the membrane-stabilized nitrate ISEs under stationary and flow conditions.	20
3. Statistical values of the measurements.	30

Comparison of Potentiometric Sensors with Amperometric Sensors for Determination of Nitrate

By: Solomon Mehretie

Advisor: Dr. Bernd Hundhammer

ABSTRACT

A potentiometric sensor based on a membrane-stabilized interface between two immiscible liquids has been developed. It has been tested in both stationary and flow conditions for the determination of nitrate. The selectivity of the sensor based on the concept of ion exchange has been studied. On the other hand, an amperometric flowthrough sensor based on nitrate transfer across the interface of two immiscible electrolyte solutions has been developed. The sensor was applied in a flow injection system for the determination of nitrate ion in tap water. The results from both sensors (potentiometric and amperometric) are in the same range (2.5 - 4.5 mg l⁻¹). The results also agreed with measurements conducted using a UV-detector.

1. INTRODUCTION

Nowadays analysis of anions is of interest due to environmental and agricultural reasons. Too much accumulation of ions such as nitrate and fluoride in the environment increasingly become a danger for human health and animal life. Nitrate ions in water and food are of concern because under condition prevailing in human digestive system they can be converted to nitrosamines [1], which are compounds suspected of initiating cancer. Furthermore nitrates can be released into water body in large amounts due to the use of fertilizers, and via runoff of manure from poorly managed livestock farms. The most noticeable effect of this is stimulation of biological activity such as formation of green algae. Such waters are difficult to treat to an acceptable standard for domestic purposes.

Nitrate poisoning is widespread and caused by large accumulation of nitrates in plants due to abnormal synthesis of nitrates into amino acids and proteins. A nitrate content of 1.5% or more of plant's dry weight is considered lethally toxic [2]. In some cases, plants can accumulate as much as 10% or more. In the rumen of cattle, nitrates are converted to nitrites which are absorbed into the bloodstream and change hemoglobin into methemoglobin which cannot carry oxygen. This is the cause of death of many cattle yearly.

A number of methods have been developed to determine the amount of nitrate in natural samples. The most frequently method is reducing nitrate to ammonia using Devarda's alloy. Ammonia is then determined by titration after distillation [3]. Another alternative method is reducing nitrate to nitrite when a sample is run through a column containing amalgamated cadmium filings. The nitrite thus produced is determined by diazotizing with sulfanilamide and coupling with N-(1-naphthyl)-ethylenediamine to form a highly colored azo dye that is measured colorimetrically [4]. These methods, however, are not free from interfering ions such as nitrite in the original sample solutions and time consuming. For the last twenty five years or so easier and much more fast potentiometric methods [5-8] and amperometric

methods [9] have been used.

As indicated by Koryta [10] in the introduction of his review, of the four physical models of a membrane, two of them are: the thick liquid membrane, and the interface between two immiscible electrolyte solutions (ITIES). The former which comprises two interfaces (water/oil) is mainly used in ion-selective electrodes (ISEs) by keeping internal interface constant. While the latter represented by a single interface of two immiscible electrolyte solutions which is applicable in various voltmmatric techniques.

Liquid membranes containing dissolved ion exchanges were first used by Sollner and Shean [11] but these show only selectively toward the sign of the ion charge rather than the kind of ion. Even so, they have proved useful and are capable of development as, for example in the divalent cation exchanger electrode [12]. A more general theory of ion transport in liquid membrane was proposed by Sandblom *et al.* [13]. The theory is helpful for interpretation of ISEs of this type, and predict the observed linear relationship between selectivity of the ISE and the ion-distribution coefficients. However, the theory is unsuccessful in explaining the observed fact that the experimental selectivity coefficients vary with the experimental conditions under which it is determined [14]. Still the way selectivity coefficient varies with the activity of the interfering ions was remain unanswered [15].

Midgley [16] has made an attempt to interpret this fact in terms of the concentration polarization of the ions in the solution just outside the membrane. This treatment presumes the validity of the basic assumption implied in the Sandblom *et al.* theory [13], that of the steady state of the ion transport throughout the liquid-membrane. This assumption, however, is not realistic when the membrane is not thin enough. When a relatively thick membrane is brought into contact with a sample solution, the composition of the internal interface would remain unchanged unless a sufficiently long time elapses, while the compositions in the vicinity of membrane-sample solution change with time due to the ion-transfer reactions

across the interface, resulting in concentration polarization on both sides of the interface [17]. So it is necessary to examine the ion-transfer processes occurring at the membrane-sample solution interface for the understanding of potentiometric responses of liquid state ISEs.

In this regard, Kakiuchi and Senda [17] proposed a quantitative theory on the concept of mixed ion-transfer potential in the presence of interfering ion, at the liquid membrane/sample solution interface. The theory expresses the potential and selectivity coefficient of the electrodes as functions of three factors: difference in the Standard Ion-Transfer Potential between primary and interfering ions, concentration ratios of primary and interfering ions, and diffusion coefficient ratio of these ions. Experimentally, the theory was also verified by Kakiuchi *et al.* [18] using liquid state ISEs.

A more simplified relation between potential and selectivity coefficient was shown by Koryta [12] even though it was derived earlier than Kakiuchi and Senda [17]. He made simplification by assuming that no ion association occur within the solvents. This can be usually achieved by using solvents having high dielectric constants so that ions are effectively separated.

On the other hand, ion transfer process between immiscible electrolyte solutions have been extensively studied using various electrochemical techniques as reviewed by Koryta [10, 19]. In his review, the aqueous phase contains a base electrolyte lithium chloride while that of non-aqueous phase contains tetrabutylammonium tetrphenylborate [TBA⁺TPB⁻]. Since these electrolytes have very high negative and positive values of standard Gibbs energies of transfer from non-aqueous solvent to aqueous solvent, respectively, a suitable potential range is formed. This potential range is usually called potential window which is limited by the transfer of the ions of the base electrolyte across the interface.

Within a potential window, ion transfer of the less hydrophilic and hydrophobic ions can be studied using voltammetric methods [19]. However, using TBATPB in the organic phase, it is not possible to extend towards the negative value of a potential range because of transfer of TBA⁺ ions from non-aqueous to aqueous phase. Extension of this range towards negative values by substituting TBA⁺ ions by crystalviolet ions [20], and by tetraphenylarsonium ions [21] can solve the problem. Consequently, it is possible to investigate relatively high hydrophilic ions such as iodide and nitrate.

The other important circumstance that has to be taken in consideration in the study of ion transfer across ITIES is that these supporting electrolytes should be completely dissociated in the organic solvent. This can be achieved by using polar non-aqueous solvent. The most commonly used hitherto are nitrobenzene and 1,2-Dichloroethane. The choice of nitrobenzene mainly results from the following reasons [22]: very low solubility of water in nitrobenzene (0.34% by weight), low electrical resistance, good solubility of various chemical compounds, high permittivity (35.96), large specific density (1.2 g cm⁻³), and low vapour pressure.

The other problem associated with the analytical application of the aqueous/non-aqueous interface as an amperometric sensors (or voltammetric sensors) like that of potentiometric sensors is the mechanical instability of the interface. The two most promising approaches so far utilized in the construction of voltammetric sensors are well known methods used in the construction of liquid state ISEs [11]. The stabilization of the organic phase by gel formation with PVC has been used [23, 24] and employed for the development of voltammetric sensors. A second possibility for stabilizing the interface is to insert a porous membrane between the two liquid phases. This method was first used by Ross [25] for constructing liquid state ISEs and was shown by Hundhammer *et al.* [26] to be well suited for voltammetric studies of ion transfer across the interface.

Furthermore, for analytical application of amperometric sensors it is advantageous to keep the thickness of the diffusion layer constant. This requirement is met by wall-jet arrangement of the sensor [27] in a flow injection system. The wall-jet arrangement for investigation of ion transfer across ITIES was applied [28, 29] for analytical purpose. The flow injection analysis (FIA) was first introduced by Ruzicka and Hansen [30] in 1975. This method was applied [29] in order to simulate the conditions of ion chromatography. Besides FIA technique has been used for the determination of diffusion coefficient [31] using amperometric sensors.

The selectivity of amperometric sensors is governed by the standard Gibbs energies of partition of the individual ions between water and the organic solvent. Besides it has been shown by Hundhammer and Wilke [29] that the selectivity of the sensors can be varied by the potential difference applied across the aqueous/non-aqueous interface.

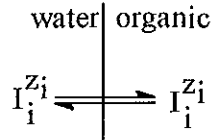
In general, potentiometric methods have the advantage of being faster and easier to apply in chemical analysis despite its logarithmic dependance of the potential on concentration. Where as, amperometric methods have the advantage of having a linear relation between current and concentration and a lower detection limit. But so far there has not been any comparison made between these two methods. It is therefor the aim of this thesis:

- To determine the nitrate ion potentiometrically and amperometrically under stationary and flow injection conditions.
- To comare potentiometric sensor with that of amperometric sensor.
- To compare the results of these sensors with UV-detector results.

2. THEORY

2.1. POTENTIOMETRIC RESPONSES OF LIQUID STATE ISEs

When a system composed of two immiscible liquids (water/oil) contains an ion I_i which is partitioned between the two phases, the equilibrium can be represented as



where z_i refers to the charge of the ion under consideration.

In the equilibrium state, the electrochemical potential of each ion is equal, thus

$$\mu_i^{o,w} + RT \ln a_i^w + z_i F \phi_i^w = \mu_i^{o,o} + RT \ln a_i^o + z_i F \phi_i^o \quad (1)$$

where $\mu_i^{o,w}$ and $\mu_i^{o,o}$ stand for standard potentials of ions, a_i^o , a_i^w represent their activities, ϕ_i^o , ϕ_i^w are Galvani potentials of the phases, and R, F, and T have the usual meanings.

The Galvani potential difference between the two phases is obtained by rearranging eq. (1) as

$$\Delta_o^w \phi_i = \Delta_o^w \phi_i^o + \frac{RT}{z_i F} \ln \frac{a_i^o}{a_i^w} \quad (2)$$

where $\Delta_o^w \phi_i^o$ is the standard Galvani potential difference. The standard transfer energy of an ion from the aqueous phase (w) to the nonaqueous phase $\Delta G_{tr,i}^o$ (w→o) denoted in abbreviated form by the symbol $\Delta_w^o G_i^o$ is the difference of the standard Gibbs energies of solvation in both phases.

$$-\Delta_o^w G_i^\circ = \Delta_w^\circ G_i^\circ = \Delta G_{tr,i} = \Delta G_s^\circ - \Delta G_h^\circ \quad (3)$$

where ΔG_s° and ΔG_h° are the standard Gibbs energies of solvation and hydration, respectively.

If a_i° remains constant then $\Delta_o^w \phi_i$ varies in a Nernstian fashion with the activities of species I in solution. We can write

$$\Delta_o^w \phi_i = K - \frac{RT}{z_i F} \ln a_i^w \quad (4)$$

where K is:

$$\Delta_o^w \phi_i^\circ + \frac{RT}{z_i F} \ln a_i^\circ$$

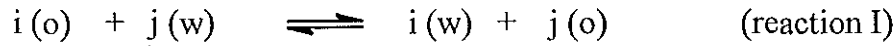
Eq. (4) shows a variation of 59/n mv per decade of variation in activity at 298 K.

However, no ion-selective electrode responds exclusively to the primary ion. If the interfering ion is present along with primary ion in the solution, the electrode response will have contributions from both the primary and interfering ions. The degree of selectivity of the electrode for the primary ion (I) with respect to an interfering ion (j) is expressed by the potentiometric selectivity coefficient ($k_{i,j}^{pot}$). Thus eq. (4) can be rewritten as

$$\Delta_o^w \phi_i = K - \frac{RT}{z_i F} \ln \left(a_i^w + \sum_j k_{i,j}^{pot} a_j^{\frac{z_i}{z_j} w} \right) \quad (5)$$

When an electrode is very selective for primary ion in comparison with interfering ion, then $k_{i,j}^{pot}$ will be much less than unit. Conversely, if the electrode responds preferentially to interfering ion rather than primary ion, $k_{i,j}^{pot}$ will be greater than unity.

In membrane stabilized liquid/liquid ISEs, selectivity coefficient can be computed by considering ion exchange reaction between primary and interfering ions in the two phases in the form:



At the interface, the thermodynamic equilibrium condition holds for the reaction from which the equilibrium ion-exchange constant or in this case selectivity coefficient is given by

$$K_{ij}^{pot} = \frac{C_i(w)C_j(o)}{C_i(o)C_j(w)} = \frac{K_{pj}}{K_{pi}} \quad (6)$$

where K_{pj} and K_{pi} are partition constants which can be determined from thermodynamic equilibrium relation ($-\Delta G^\circ = RT \ln K_p$).

2.2 THEORY OF THE SENSOR RESPONSE

Fig. 1 shows a model of a membrane stabilized interface. The water/oil interface is located at $x = 0$, the membrane extends to $x = a$ and the empirical stagnant diffusion layer δ extends from $x = a$ to $x = \delta$.

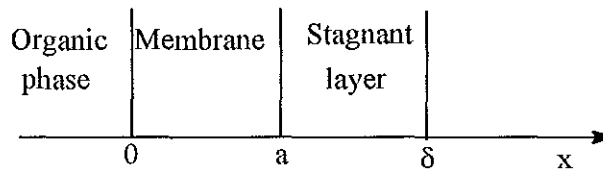


Fig. 1. Schematic diagram of a membrane-stabilized interface

The wall-jet arrangement of the sensor ensures the establishment of a hydrodynamic boundary layer within which a hypothetical stagnant diffusion layer δ , adjacent to the hydrophilic membrane, is assumed to exist. This simplification of the actual convective diffusion outside the membrane to molecular diffusion enables us to obtain an operational solution for the response dynamics of membrane-stabilized interface [31]. The empirical average thickness of their diffusion layer is given by [32]

$$\delta = 2.28 D_w^{1/3} a^{1/2} \nu^{5/12} R^{5/4} V^{-3/4} \quad (7)$$

where a is the diameter of the nozzle, ν is the kinematic viscosity, R is the radius of the sensor, V is the volume flow rate and D_w is the diffusion coefficient in water of the ion under investigation.

We consider region $0 < x < \delta$ with zero initial concentration, no flux of concentration at $x = 0$, and $x = \delta$ maintained at bulk concentration (C_b) for $t = 0$. This can be achieved by concentration-step technique which is experimentally obtained by changing the flow of the carrier solution to carrier solution containing the ion under investigation at the desired concentration. Under this condition the diffusion problem can be solved by Laplace transformation [33].

After inversion of the Laplace transform to the time scale, the concentration as function of space-time is given by

$$C(x,t) = C_b \sum_{n=0}^{\infty} (-1)^n \operatorname{erfc} \frac{(2n+1)L-x}{2(Dt)^{1/2}} + C_b \sum_{n=0}^{\infty} (-1)^n \operatorname{erfc} \frac{(2n+1)L+x}{2(Dt)^{1/2}} \quad (8)$$

At $x = 0$, this expression can be shorten as

$$C(\zeta,t) = 2C_b \sum_{n=0}^{\infty} (-1)^n \operatorname{erfc} \frac{2n+1}{2\zeta^{1/2}} \quad (9)$$

where ζ is a dimension less parameter (Dt/l^2).

2.3. AMPEROMETRIC RESPONSE OF THE SENSOR

In the diffusion layer it was postulated that diffusion alone controlled the transfer of substances to the electrode. Outside the layer diffusion was negligible and the concentration of electroactive species was maintained at the value C_b by convective transfer. Nernst assumed a linear concentration gradient in the diffusion layer and he derived the current-concentration relation as follows. The rate(r) of transfer of electroactive species per unit area is given by [34]

$$r = D_w \frac{C_b - C_{x=0}}{\delta} \quad (10)$$

the current flow then is

$$i = nFA D_w \frac{C_b - C_{x=0}}{\delta} \quad (11)$$

where A is the area of the electrode.

But concentration at $x = 0$ is zero. Substituting the the thickness of diffusion layer given in eq. (7) into eq. (11), the limiting diffusion current (i_l) is given by

$$i_l = k z_i D_w^{2/3} C_b \quad (12)$$

where $k = 1.38 F \nu^{-5/12} a^{-1/2} R^{3/4} \nu^{3/4}$.

In the presence of interfering ions, each interfering ion contributes to the current in addition to the primary ion current. Thus the total current is given by

$$I = k \sum b_i C_i \quad (13)$$

where b_i is the partial sensitivity of the i^{th} ion in the sample.

The partial sensitivity of the individual can be obtained by rearranging the following equation

$$\Delta_o^w \varphi_i = \Delta_o^w \varphi_{1/2,i} + \frac{RT}{z_i F} \ln \frac{i}{i_i - i} \quad (14)$$

where $\Delta_o^w \varphi_{1/2,i}$ is the half-wave Galvanic potential difference.

$$b_i = \frac{z_i D_w^2 / 3}{1 + \exp\left[\frac{z_i F}{RT} (\Delta_o^w \varphi_{1/2,i} - \Delta_o^w \varphi)\right]} \quad (15)$$

It can be seen from eq. (15) that the partial sensitivity of the sensor for a certain ion is determined by the difference between the applied Galvanic potential difference and the respective half-wave Galvanic potential difference [29].

2.4. FLOW INJECTION ANALYSIS

Flow injection analysis is based on a combination of three principles: sample injection, controlled dispersion of the injected sample zone, and reproducible timing of its movement from injection point toward and into the detector. The physical process of material dispersion is due to the hydrodynamic process taking place in the flowthrough system, based on the combined effect of convection and diffusion. When convection dominates over diffusion, excessive dispersion occurs in the flowthrough stream due to axial distribution of the sample elements. This can be avoided by promoting radial dispersion which can be achieved by using turbulent flow, by diffusion alone, or by a combination of these effects.

Generally, the degree of dispersion is governed by the injected sample volume, the flow rate, the channel length, and geometry. For a one channel system, the more the sample volume is, the lesser is the dispersion of the sample through the channel. As result of which

the peak height of measurement gets enhanced. On the other hand, the dispersion of the sample decreases with decreasing flow rate. In other words the magnitude of signal decreases at higher flow rate. With regard to the length of the channel, Rucizka and Hansen [28] stated that '*the dispersion of the sample zone increases with square root of distance traveled through an open narrow tube.*' However, this rule is valid only for straight channels. When the channels are coiled for the sake of tidiness to improve radial dispersion, the intensity of dispersion is decreased to different degrees, depending on the radius of the coil.

2.5. UV- VISIBLE ABSORPTION

When a beam of radiation of specific wavelength passes upon a substance, the energy associated with the beam may be altered by reflection, refraction, absorption and transmission processes. Most experimental measurements are concerned with elimination of, or corrections for, effects other than absorption [35].

The simplest situation with respect to the intensity of absorption is that in which the system obeys the Lambert-Beer law. In this case if I_0 is the intensity of a parallel beam of radiation incident normally on a layer of thickness b cm and molar concentration c , the intensity of the emergent beam is:

$$I = I_0 10^{-\epsilon cb} \quad (16)$$

where ϵ is molar absorptivity. Eq. (16) can be expressed in the form:

$$\log\left(\frac{I_0}{I}\right) = A = \epsilon cb \quad (17)$$

where A is the absorbance of the sample in the beam. From the last expression, it is possible to determine the amount of substance in the sample by measuring the absorbance using UV-detector.

3. EXPERIMENTAL

The experimental set up for the flow injection is schematically shown in Fig. 2a. The FI system consists of piston pump (Model 307, Gilson, France), injection port equipped with 50 or 100 μl injection loop, and a flowthrough potentiometric sensor or amperometric sensor of the wall-jet type. The potential of the potentiometric sensor was measured using a pH meter (Philips, PW 9418) and the output of the pH meter was recorded using a Model PL3 recorder.

Figure 2b shows the schematic wall-jet cell in which the potentiometric sensor or the amperometric sensor and the reference electrode were placed. The potentiometric sensor was made by dissolving μ -nitrido-bis (triphenylphosphorous)nitrate (PNPNO₃) into nitrobenzene. The PNPNO₃ was prepared as described in ref. 36. The precipitate of PNPNO₃ was filtered off and washed several times with distilled water. The precipitate was then recrystallized from water for further purification. A hydrophilic dialysis membrane (PT 125 or PT 325) (Kleinfled and Co. GmbH, Hannover, Germany) was used to stabilize the water/nitrobenzene interface. Here nitrobenzene was used after purification. Purification was done by washing nitrobenzene with 10 % H₂SO₄, 5 % NaOH and finally with distilled water until the water was neutral. A silver/silver chloride electrode with a liquid junction (0.1 M MgSO₄) served as a reference electrode in both the sample and the internal solution.

Standard solutions were prepared from a 0.1 M KNO₃ stock solution by sequential dilution with distilled water. The ionic strength of all solutions was kept constant at 0.1 by adding the required amount of magnesium sulphate. A 0.1 M MgSO₄ solution served as the carrier solution in the FI system.

In the amperometric experiment, the supporting electrolytes were 5 mM MgSO₄ in the aqueous phase and 10 mM crystal violet tetraphenylborate in nitrobenzene. The cell employed is shown in Fig. 3. A silver wire coated with silver chloride served as reference

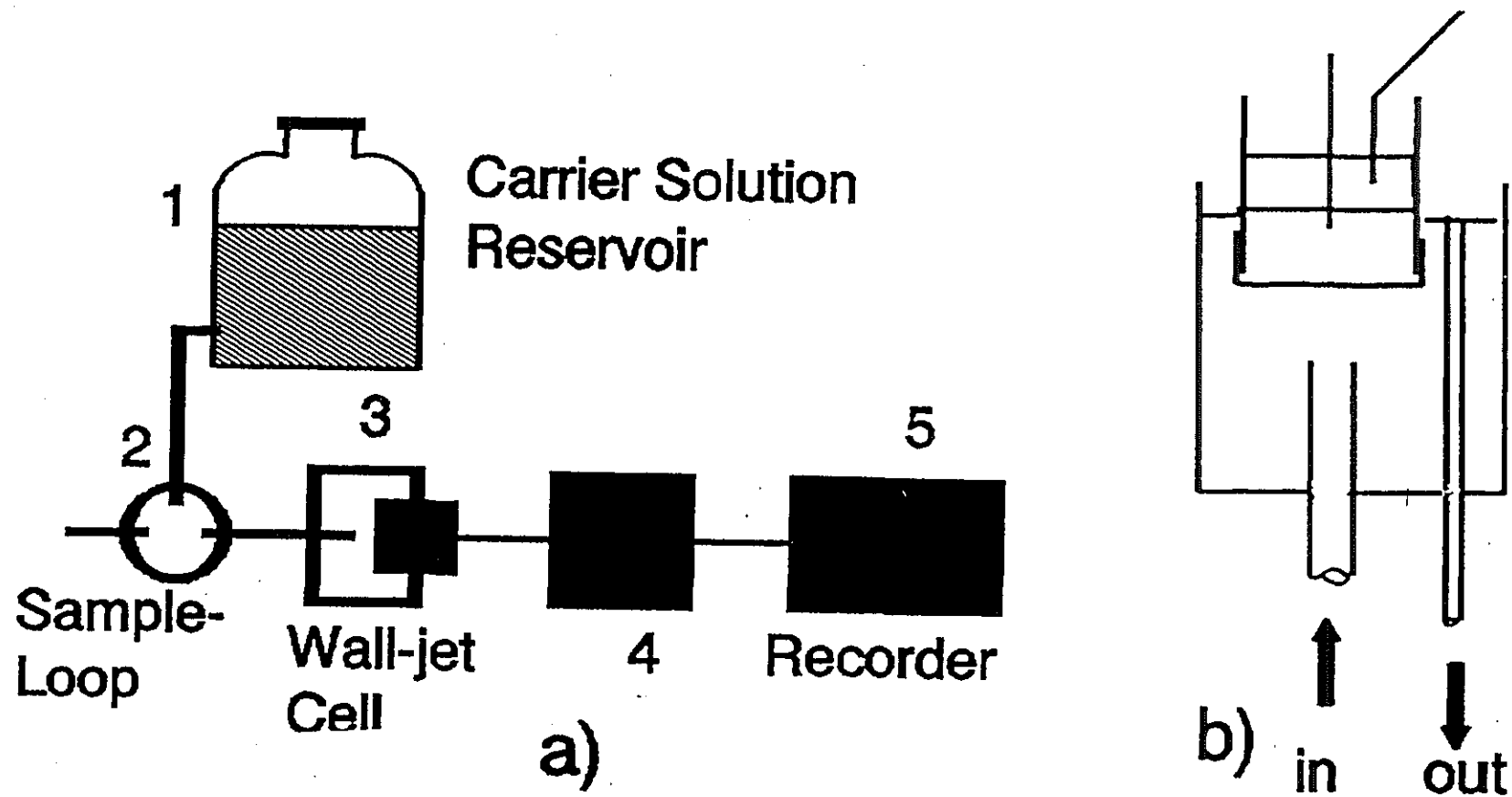


Fig. 2 a) Block diagram of the flow injection system, 4 could be pH meter or amperometric detector
 b) Schematic diagram of the wall-jet cell.

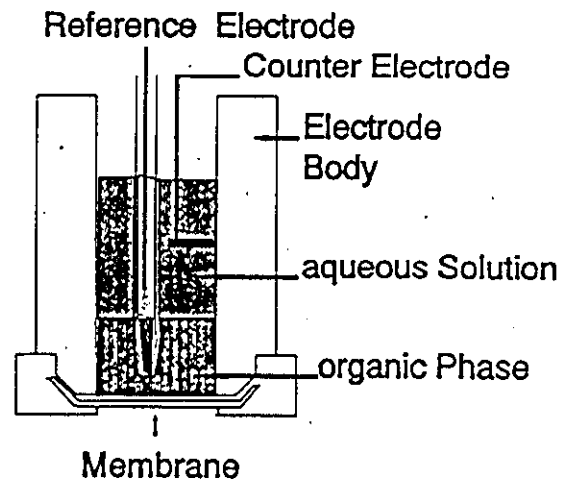


Fig. 3. Diagram of amperometric cell.

electrode in the organic phase. A silver/silver chloride reference electrode was employed in the aqueous phase. All chemicals were of analytical grade. All experiments were carried out at room temperature (20 ± 2 °C).

3.1. A MODIFIED FOUR ELECTRODE POTENTIOSTAT WITH *iR* COMPENSATION

The most serious problem in voltametric measurements at liquid-liquid interface is the control of the Galvanic potential difference across the interface. The four electrodes technique, which is commonly employed, uses two counter-electrodes to feed or to take the electric current to/from the system while the potential difference is controlled by two reference electrodes [37].

The electronic circuit of our modified potentiostat is shown in Fig. 4. OA 1 is the control amplifier of the potentiostat. The output of the differential amplifier 1 (INA 111) is at a potential proportional to the current in order to convert the potential into a current (with a $22 \text{ k}\Omega$). The voltage follower (OA 2) serves as a buffer amplifier. Since the BAS sees a current at the input to the working electrode, a resistor of $22 \text{ k}\Omega$ is inserted. Thus the current scale of the BAS can be used without correction.

The differential amplifier 2 (INA 111) controls the potential difference across the interface. The *iR* compensation is realized by setting the reference potential of the amplifier to a potential drop between the two reference electrodes. This can be done by applying part of the potential from potentiometer ($100 \text{ k}\Omega$) into the sensing input of the amplifier 2 (INA 111). OA 5 and INA 105 (2) are used as buffer amplifier. The special feature of this modified potentiostat is that the counter electrode of the aqueous phase is set to real ground. This is advantageous in solving the problem of noise created by the pump in our FI system.

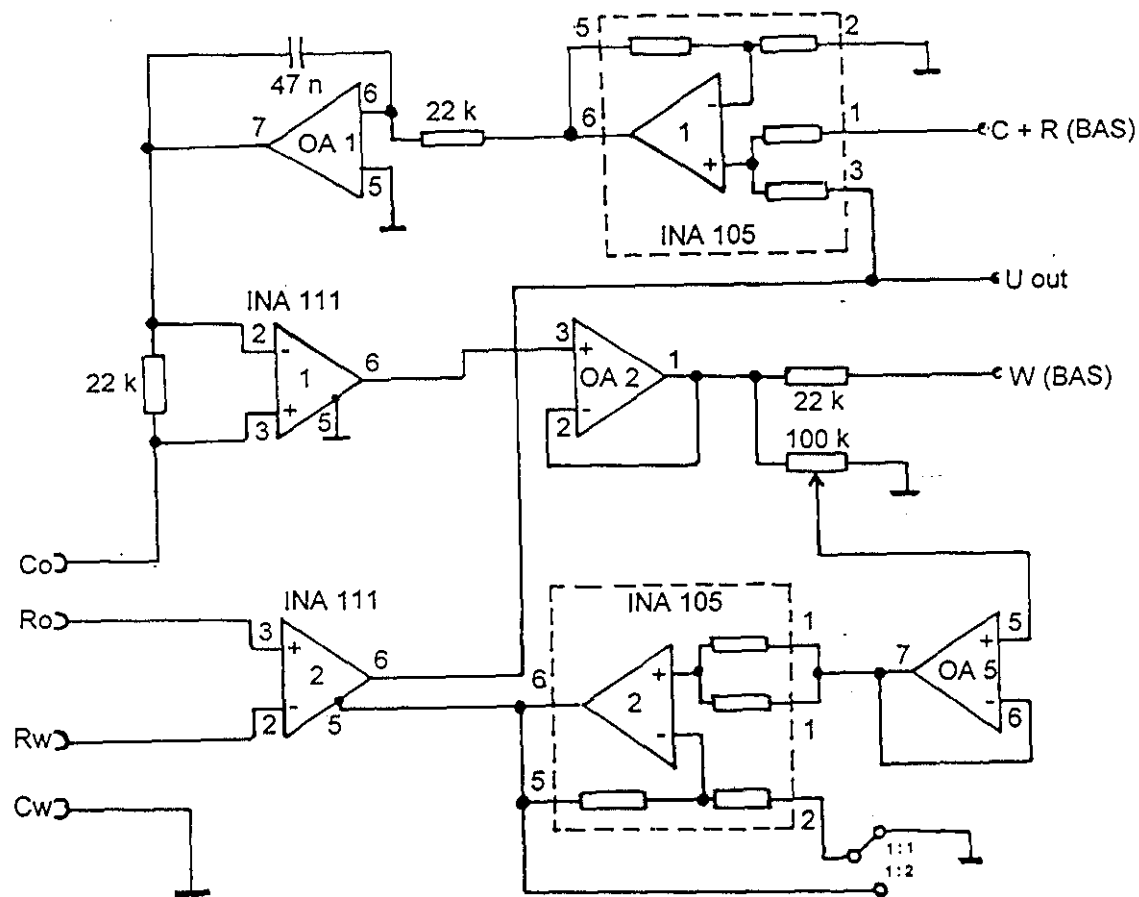


Fig. 4. Electronic circuit of the four electrode potentiostat. Co and Cw are counter electrode in the organic and aqueous, Ro and Rw are reference electrodes in organic and aqueous, respectively.

4. RESULTS AND DISCUSSION

4.1. RESPONSE BEHAVIOR OF THE POTENTIOMETRIC SENSOR

The influence of the amount of PNPNO₃ in the organic phase on the performance of the sensor was investigated first. The response characteristics at different concentrations (10 mM, 1 mM, 0.1 mM PNPNO₃) is shown in Fig. 5 and the results are given in Table 1.

Table 1. The influence of amount of PNPNO₃ in the organic phase on the performance of the sensor.

Parameter	Concentration of PNPNO ₃ in the organic phase		
	10 mM	1 mM	0.1 mM
Linear range/ M	0.1-7.5x10 ⁻⁵	0.1-1.8x10 ⁻⁵	0.1-7.5x10 ⁻⁶
Slope/ mV per decade	60.8	60.4	59.1
Detection limit/ M	5x10 ⁻⁵	10 ⁻⁵	6.5x10 ⁻⁶

As expected 0.1 mM PNPNO₃ exhibits the widest linear range and the lowest detection limit. By making the organic phase more concentrated with PNPNO₃ results a narrower linear range and a higher detection limit. Every ion in both organic (PNP⁺ and NO₃⁻ and aqueous (K⁺, Mg²⁺, NO₃⁻ and SO₄²⁻) phases participates in the partition equilibrium. But, since K⁺ and Mg²⁺ are strongly hydrated in the aqueous phase, they prefer to stay in the aqueous phase. PNP⁺ is such a big molecule that it is hardly hydrated and hence, it remains in the organic phase. The nitrate ion is partitioned in the two phases. When the concentration of the PNPNO₃ is high in the organic phase (such as 10 mM PNPNO₃), the nitrate ions leave out from the organic phase because of concentration gradient. This results poor performance of the sensor compared with the lower concentration.

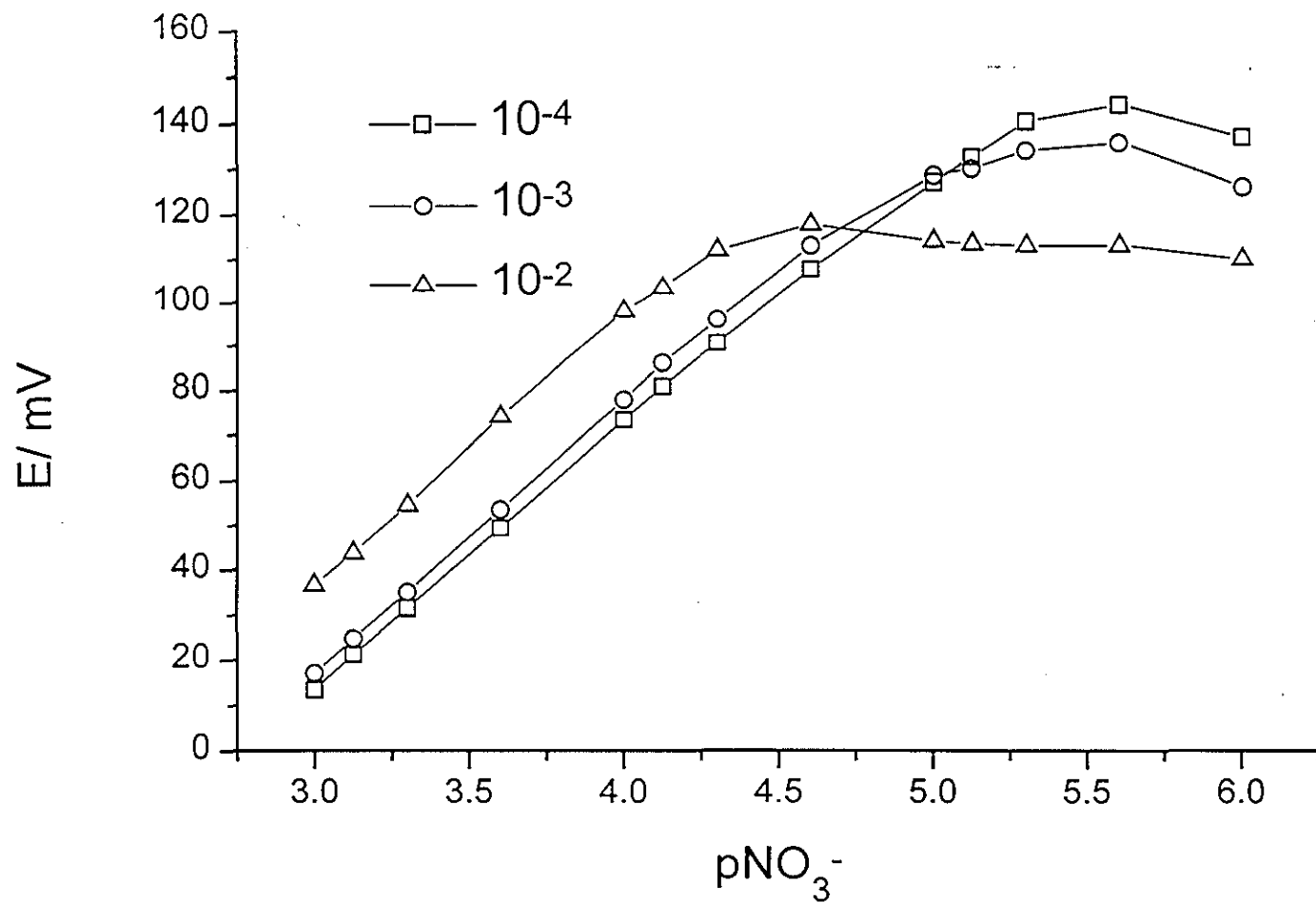


Fig. 5. Response behavior of the potentiometric sensor at different concentrations of PNPNO₃

However, further lowering of the concentration (below 0.1 mM) of PNPNO₃ gave a rather erratic response due to lowering of conductivity. When the concentration of PNPNO₃ in the organic phase gets lower, the resistance of the solvent increases. As a result, a noisy sensor was observed. For this reason the optimum concentration of PNPNO₃ selected was 0.1 mM for further investigation.

The response characteristics of the sensor under flow conditions and the stationary response are given in Table 2. The sensor response under the flow conditions exhibits a narrower linear range. The range becomes even more narrower when the flow rate is getting higher. These observations can be explained as follows. Since the contact time of the sample over the surface of the sensor is very short compared with the time constant of the sensor, the equilibrium condition is not reached during measurement. As a result, the magnitude of the signal is very much lower than the stationary state measurement.

As seen in Fig. 6, it is difficult to get the detection limit of FI measurement. This is because of the background nitrate ions present in the wall-jet cell. But it is expected to be lower than the stationary condition for the same reason mentioned in the preceding paragraph.

Table 2. The performance of the membrane stabilized nitrate ISEs under stationary and flow conditions.

Parameter	Electrode	
	Stationary state	Flow system
Linear range/ M	0.1 - 1.8x10 ⁻⁵	0.1 - 10 ⁻⁴ (2) 0.1 - 4x10 ⁻⁴ (4)
Slope/ mM per decade	57.6	57.6
Detection limit/ M	10 ⁻⁵	-----

Numbers in the bracket are flow rates in ml min⁻¹.

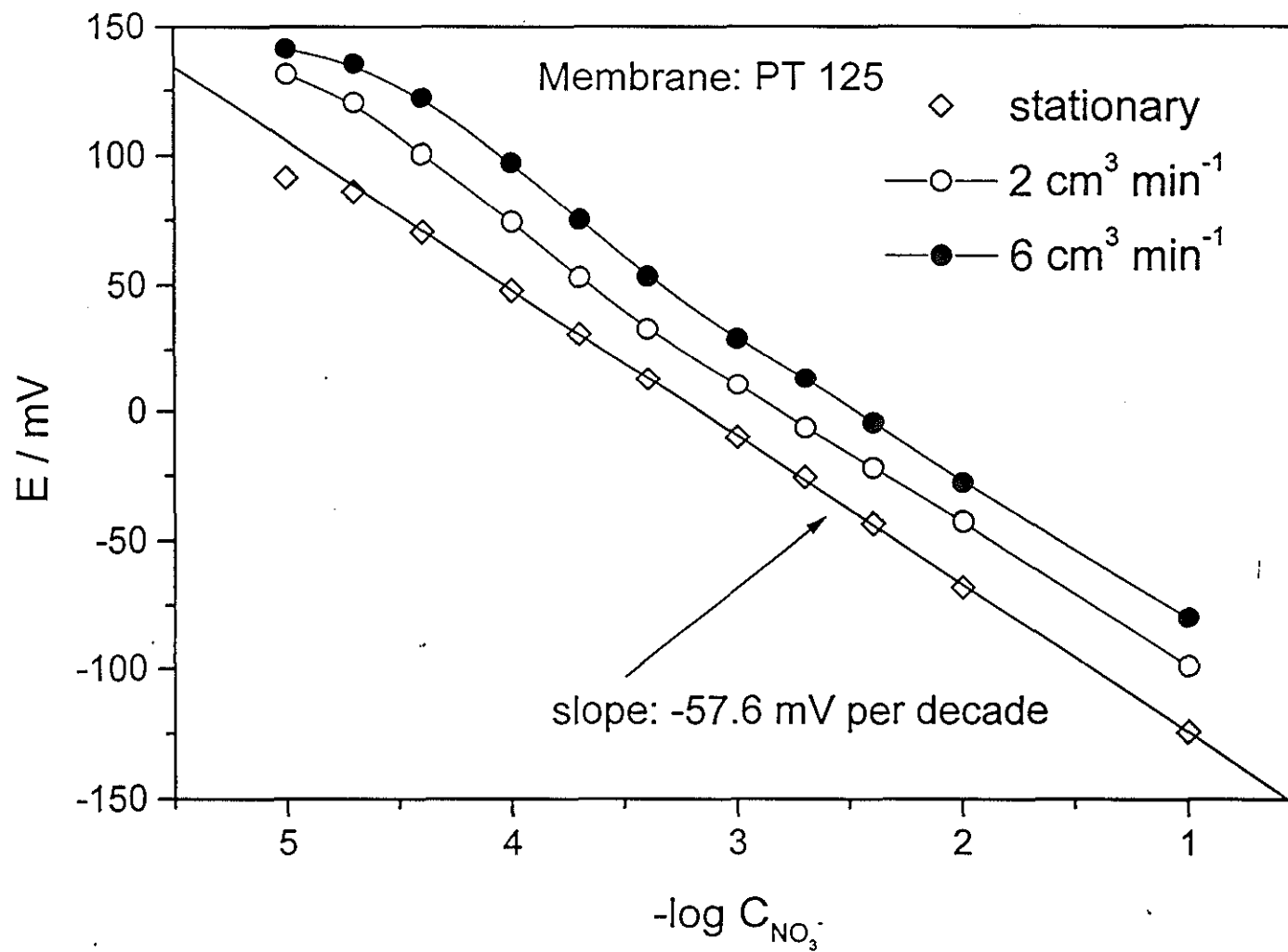


Fig. 6. Response of the potentiometric sensor under flow and stationary conditions

The response behavior can be also evidently explained by considering the theoretical response of the sensor as derived above in the theory part. In the FI technique, concentration pulses are considered. Here concentration pulses can be approximated experimentally by injecting a small amount of ion under investigation into a carrier stream, keeping the distance between the sample loop and the interface of the sensor short in order to avoid excessive dispersion of the sample with in the carrier solution. When a concentration pulse is applied, eq. (9) can be rewritten as:

$$\frac{C(0,\zeta)}{C_b} = 2 \left[\sum_{n=0}^{\infty} (-1)^n \operatorname{erfc} \frac{2n+1}{2\zeta^{1/2}} - \sum_{n=0}^{\infty} (-1)^n \operatorname{erfc} \frac{2n+1}{2(\zeta-\zeta_p)^{1/2}} \right] \quad (18)$$

where ζ_p is dimensionless pulse length.

Based on eq. (18), the dependence of concentration pulses on the pulse length was drawn in Fig. 7. The longer the pulse length, the closer the approach to concentration step response (or steady state response). In other words, shorter pulse length results in smaller magnitude of signal of the sensor. This is the reason for lowering of the detection limit and narrowing of the linear range in the FI system.

4.2. RESPONSE BEHAVIOR OF AMPEROMETRIC SENSOR

The dependence of the peak current on the potential difference is shown in Fig. 8. When the applied potential extends to the negative values, the peak current increases due to the transfer of nitrate ion from the aqueous to the organic phase. But at some potential range, the current starts to be independent of the potential applied. This region of current is called limiting current which depends on the concentration of the ion being transferred across the interface.

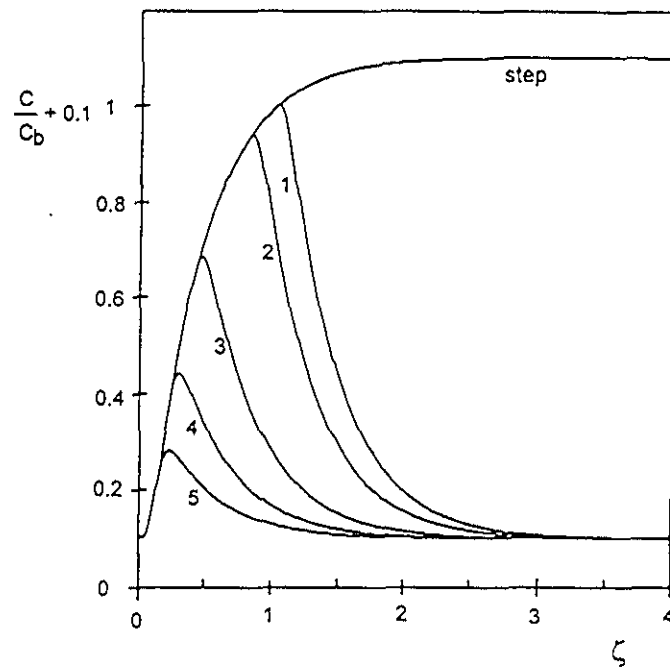


Fig.7. Calculated concentration change at a membrane stabilized interface of a liquid state ISE under flow conditions. The dimensionless pulse length (ζ_p) of the concentration pulses are 1: 1, 2: 0.8, 3: 0.4, 4: 0.2, and 5: 0.1.

It appears that the magnitude of the limiting current is lowered when the iR compensation was not made. Without the iR compensation, it is not the intended potential used but it is the apparent potential which is lower than the applied potential. This is due to the fact that part of the applied potential is dropped by the solution resistance. As a result, the magnitude of the limiting current without iR compensation is lower than with that of the limiting current with iR compensation. This indicates that it is essential to make iR compensation in determining the exact amount of the ion under investigation.

Figure 9 shows the calibration graph of nitrate at zero potential. Making the potential too large negative causes turbidity at the interface and subsequently destroy the membrane by forming a crystalviolet nitrate precipitate. The partial sensitivity obtained from the slope of the calibration graph was $2.22 \text{ nA l } \mu\text{mol}^{-1}$.

The detection limit is defined as the concentration or amount corresponding to the measurement level 3σ units above the value of zero analyte as recommended by Analytical Method Committee [38]. The quantity σ is the standard deviation of the response of the field blank which defined as a hypothetical sample containing zero concentration of analyte. The σ value obtained from our flow system was 0.92 nA as indicated in Fig. 10. Using the definition, the detection limit for the amperometric sensor was found to be $1.245 \mu\text{mol l}^{-1}$. This value is by far smaller than that of potentiometric sensor.

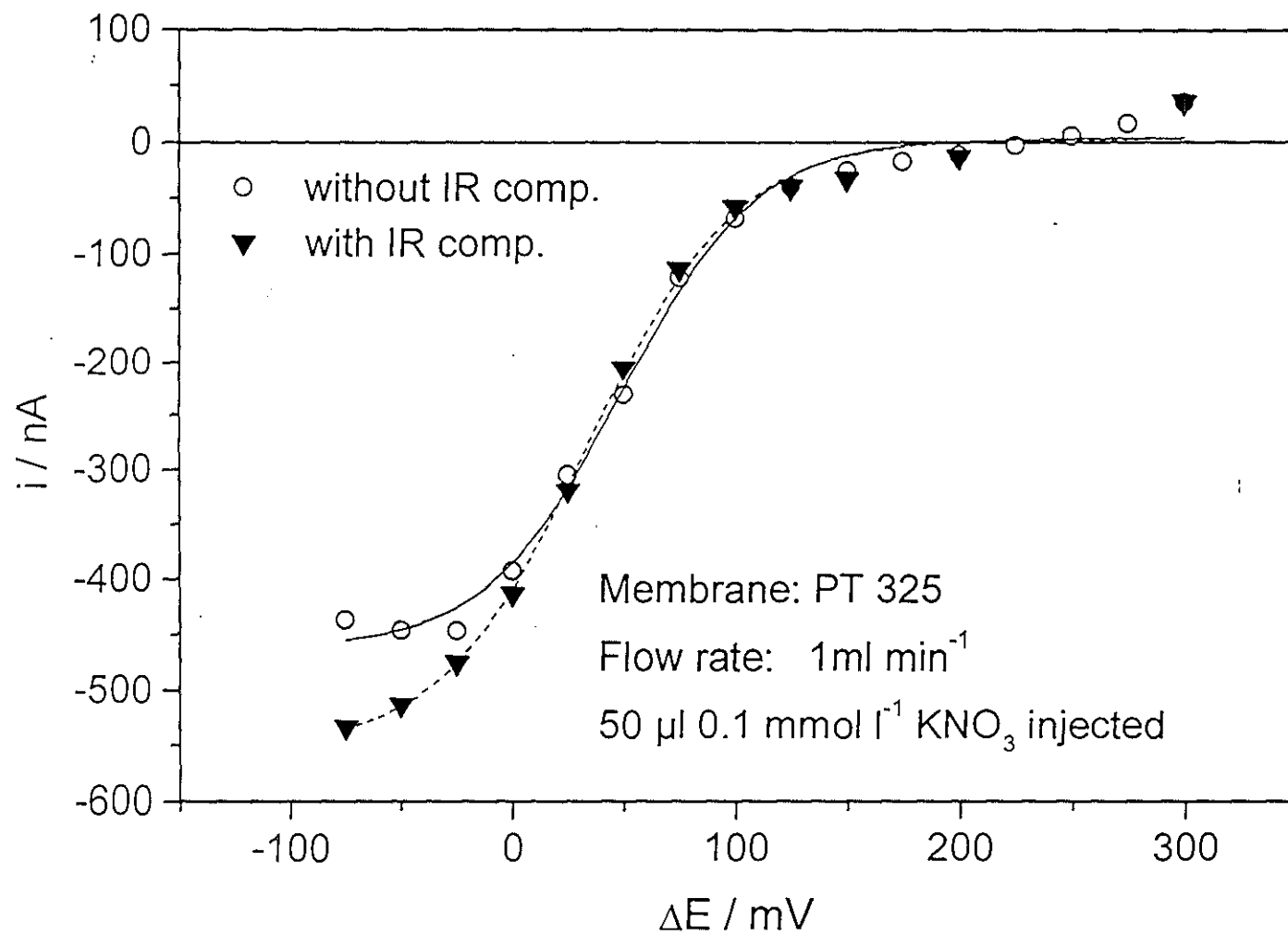


Fig. 8. Dependence of the peak current on the applied potential difference.

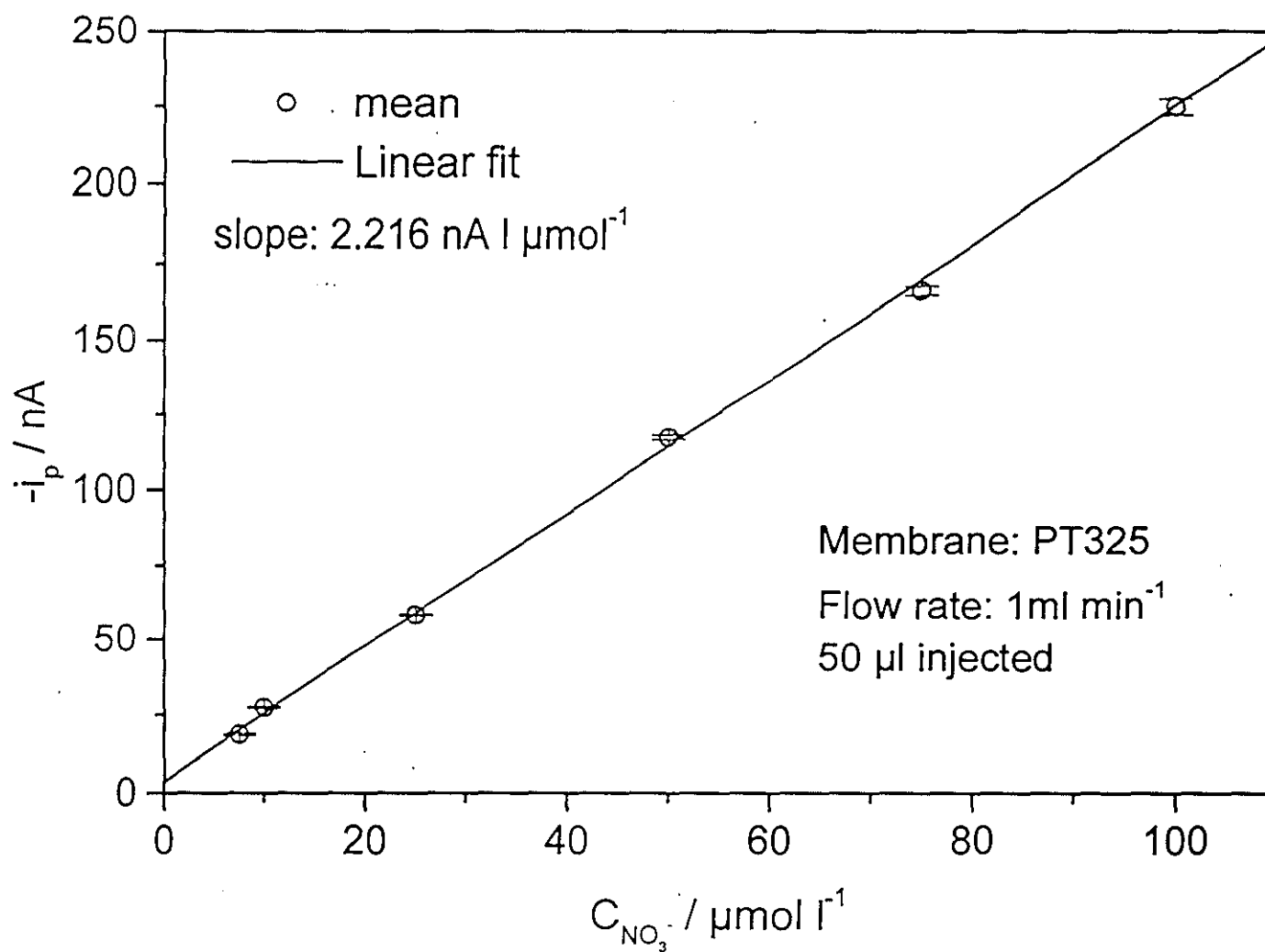


Fig. 9. Calibration graph of nitrate ion transfer at $E = 0 \text{ V}$ under flow system

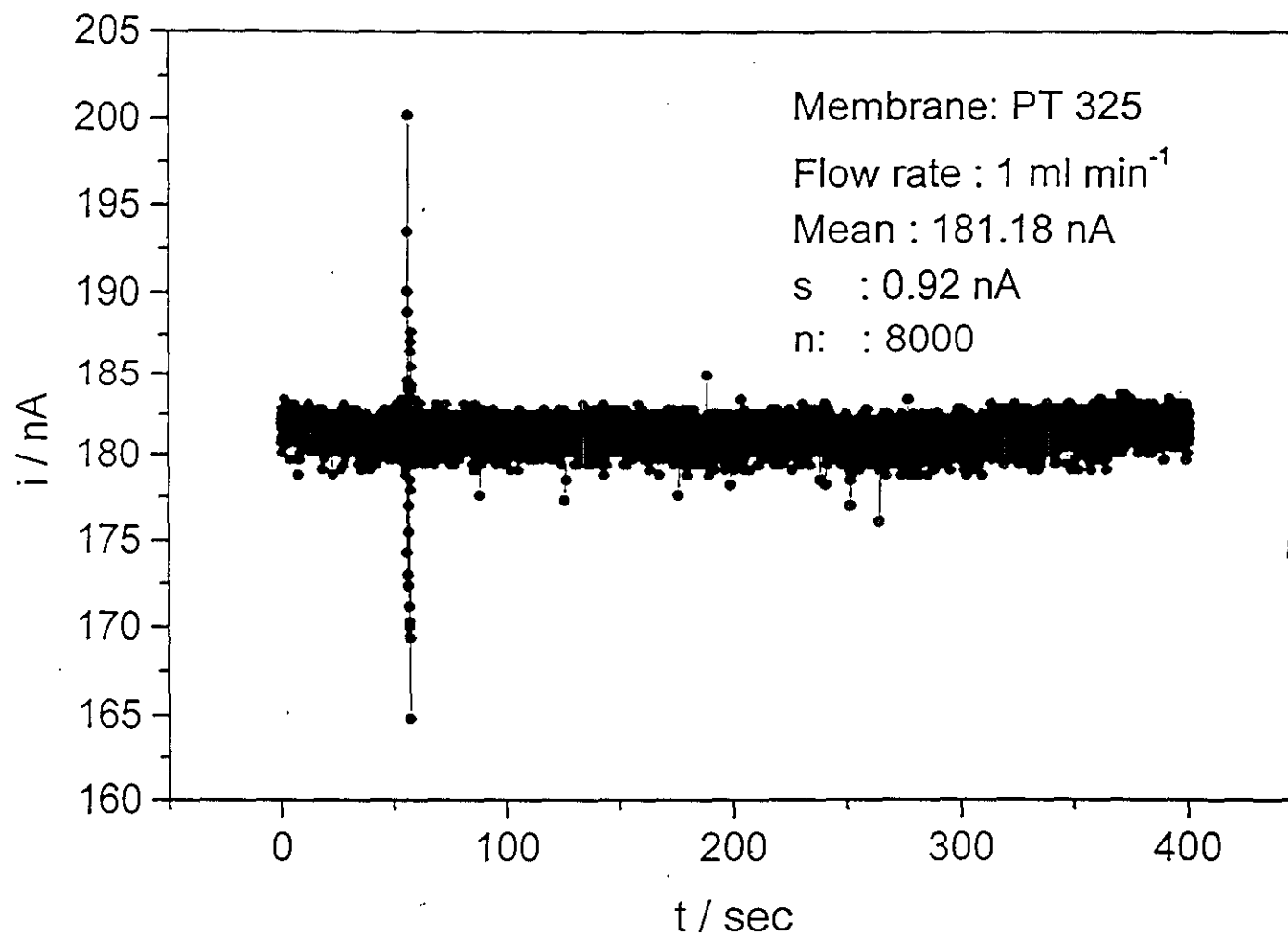


Fig. 10. Instrument response for zero analyte concentration under flow system.

4.3. DEPENDENCE OF PEAK POTENTIAL ON THE FLOW RATE

The dependence of the peak potentials of the nitrate ion on the flow rate is shown in Fig. 11. When the flow rate is small (such as 1 ml min^{-1}), 54.22 % of the steady state response is reached. On the other hand, when the flow rate is getting higher (for instance 10 ml min^{-1}), only 13.64 % of the steady state response is reached. In other words, the slower the flow rate, the closer the approach to the steady state potential response. This is because of increasing contact time of the sample with the electrode. Higher flow rates resulted in smaller peak potentials because of the shorter time of contact for diffusion of the nitrate ion into the membrane.

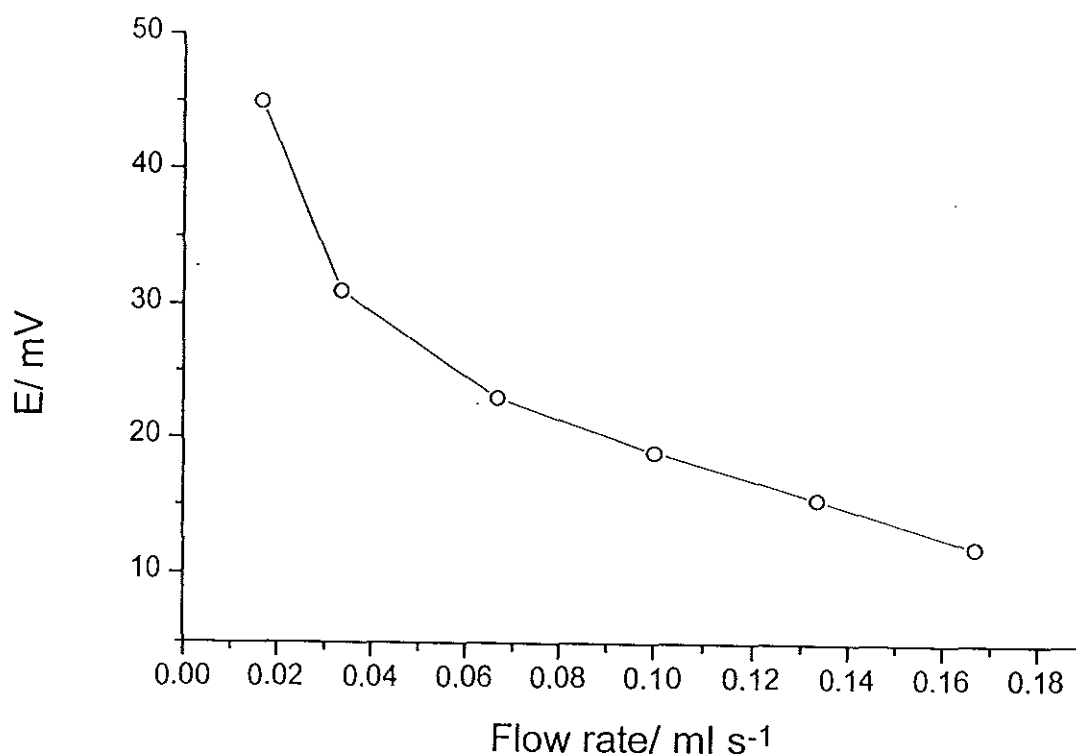


Fig. 11. Dependence of FI-peak potential for nitrate ion on the flow rate
Sample volume: $50 \mu\text{l}$, Carrier: 0.1 M MgSO_4 .

4.4. DEPENDENCE OF PEAK CURRENT ON THE FLOW RATE

The dependence of the peak currents for nitrate transfer on the flow rate is shown in Fig. 12. Starting from the flow rate 0.5 ml min^{-1} , the peak current is constantly decreasing as the flow rate increases. This indicates that there is a constant decrease in the transfer of the nitrate ion to the organic phase. Besides, the peak current decreases below the flow rate 0.5 ml min^{-1} . This may be due to convection in the cell.

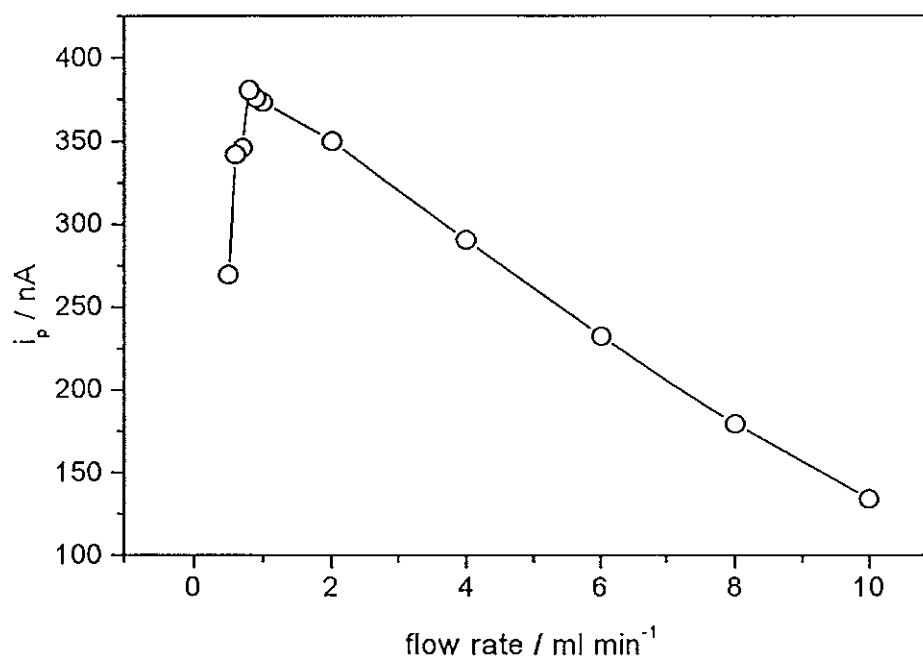


Fig. 12. Dependence of the FI-peak for nitrate transfer on the flow rate.

Sample volume: $100 \mu\text{l}$; Potential: 0 V without iR-compensation

4.5. REPRODUCIBILITY OF THE MEASUREMENTS

To test the reproducibility of the potentiometric sensor measurements, five injections were made for each concentration of the nitrate solutions. The peak potentials of each concentration of injected nitrate ions are shown in Fig. 13. The values of them were evaluated and the mean potential, the standard deviations, and the errors of the measurements are given in Table 3. The standard deviation of each concentration measurements is small, indicating quite good reproducibility of the measurements. Moreover, the error is also less than one which support the good precision of the measurements.

Table 3. Statistical values of the measurements

Conce./ mM	Mean (ΔE)/ mV	Standard deviation (\pm)	Error (\pm)
		(f = 4)	(f = 4, p = 0.95)
0.01	131.6	0.547	0.245
0.02	120.2	0.758	0.339
0.04	100.5	0.707	0.316
0.10	74.4	0.548	0.245
0.20	53.0	0.353	0.158
0.40	33.1	0.548	0.245
1.00	21.8	0.418	0.187
2.00	10.6	0.274	0.122
4.00	-6.2	0.570	0.255

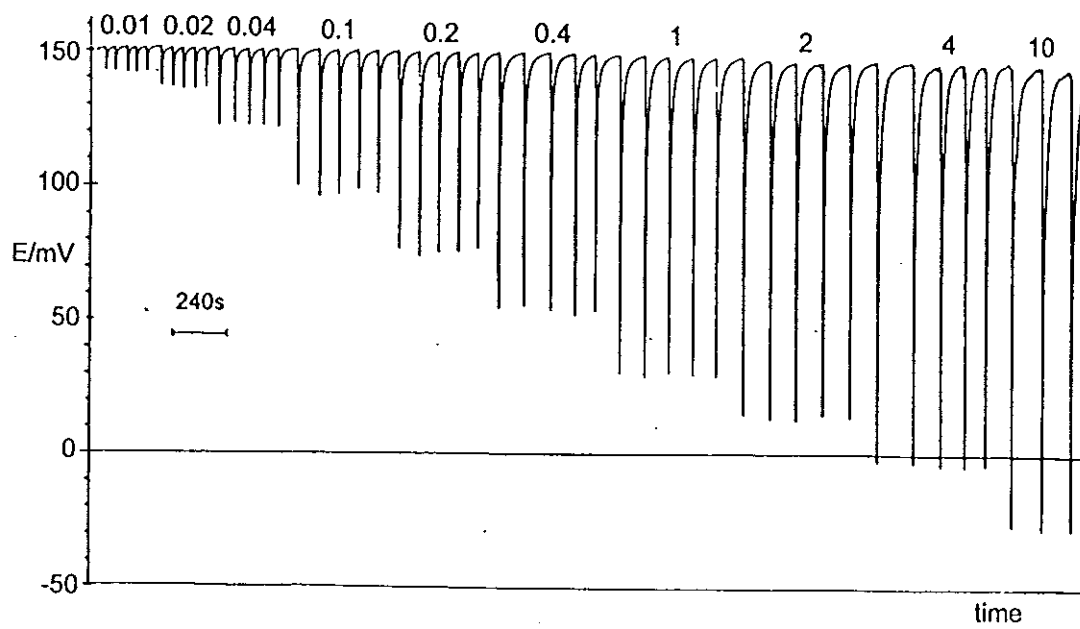


Fig. 13. Potentiometric recorder protocol of the FI system. Flow rate: 6 ml min^{-1} ; Sample volume: $100 \mu\text{l}$. Numbers on top are the concentrations of the nitrate injected in mM.

4.6. SELECTIVITY OF THE POTENTIOMETRIC SENSOR

In order to investigate the selectivity of the sensor, the response of the sensor was assessed in the presence of chloride, iodide, and perchlorate ions. These ions were selected because to study the effect of the extreme cases; that is, when the interfering ion (chloride) is more hydrophilic than the nitrate ion, and when the interfering ions (iodide and perchlorate) are less hydrophilic than the nitrate ion. Moreover, chloride is one of the ions that is present in water sample for which analytical application was applied.

The selectivity coefficient of the electrode to the chloride ion was studied by using batch injection technique. In this technique, the potential of the electrode was measured while varying the concentration of the nitrate ion via injecting small volume (1 and 10 μl) of the nitrate ion into a large volume (50 ml) of chloride solution in order to keep constant the concentration of the latter. The technique is similar to the mixed solutions method where the potential of the electrode is measured in the presence of both interfering and primary ions.

Figure 14 illustrates the response of the nitrate sensor in the presence of constant concentrations of the chloride ion. A straight line parallel to abscissa (PQ) was drawn to evaluate the concentration of the nitrate ion by extrapolating to pNO_3^- axis. P is the point at which the electrode is responding equally to both chloride and nitrate ions. This means that $a_i = k_{ij}^{\text{pot}} a_j^{z_i/z_j}$ [from eq. (4)]. Then k_{ij}^{pot} can be calculated from the activity of the primary ion (a_i) and the constant activity of interfering ion (a_j) as

$$k_{ij}^{\text{pot}} = \frac{a_i^{z_j}}{a_j^{z_i}} \quad (19)$$

Using this expression selectivity coefficient of the electrode to chloride was found to be 0.178, 0.063, 0.036 for the concentrations 10^{-4} , 10^{-3} , 10^{-2} M of the chloride solutions respectively. As seen from these figures, the selectivity coefficients changes with different

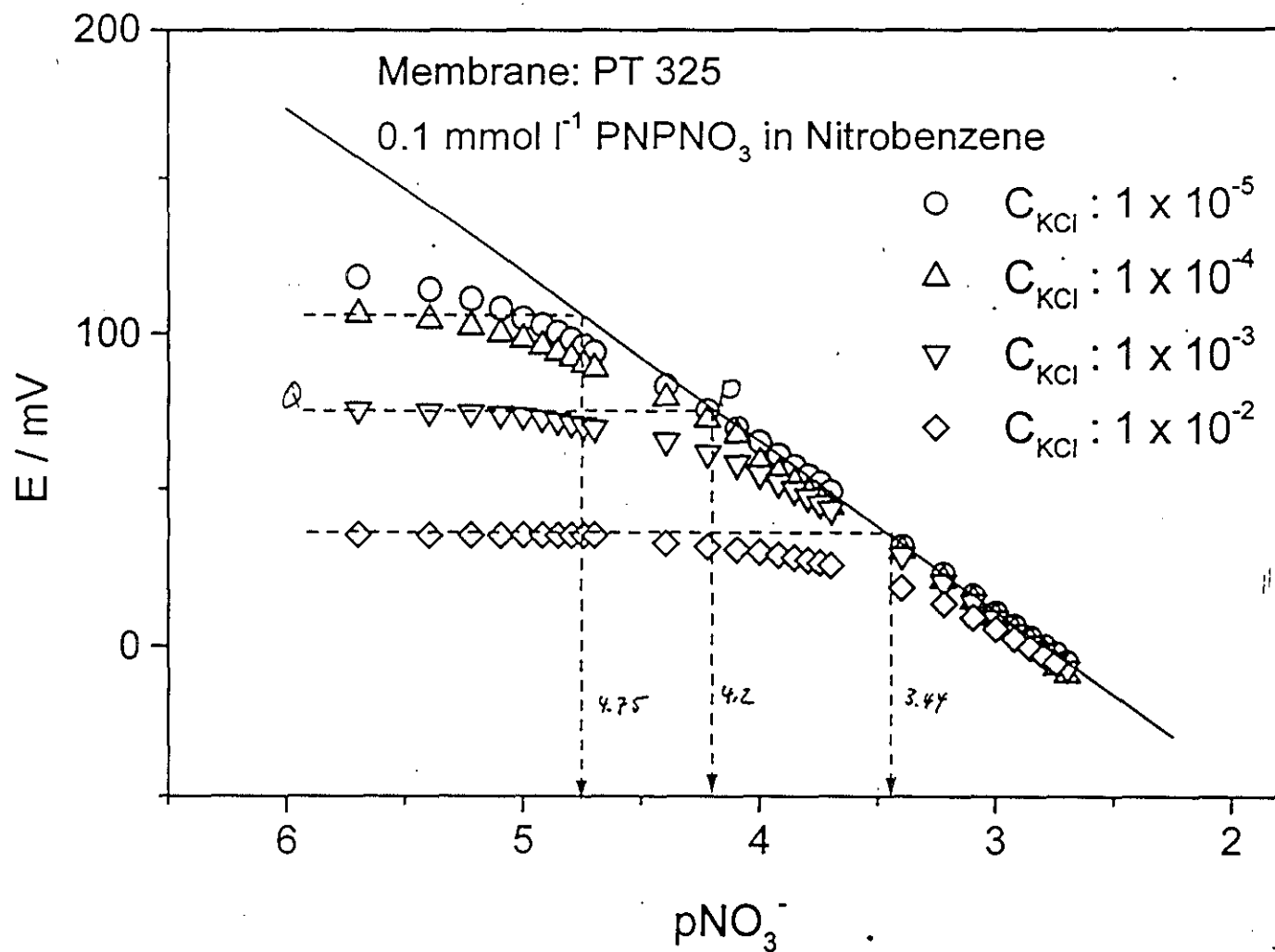


Fig. 14. Response of potentiometric sensor to chloride for different constant concentrations of KCl.

concentrations of the chloride ion. This indicates that the way the experimental conditions vary determines the selectivity coefficient. Thus a correction for the interference of chloride is rather difficult or even impossible. Based on this selectivity coefficient, the chloride ions interfere if present in greater than a ten-fold excess over nitrate ions.

The response behavior of the sensor to iodide and perchlorate ions was studied using the same technique but without the primary ion. Here, the potential was measured by injecting a small volume (1 and 10 μl) of the interfering ions into 50 ml of the supporting electrolyte solution (0.1 M MgSO_4). The selectivity coefficients to iodide and perchlorate were found to be 6.71 and 322.46, respectively, which tell that the nitrate sensor gives by far a larger response to iodide and perchlorate ion over the nitrate ion. The response behavior of the sensor to perchlorate ion described in more detail as follows.

The potential versus concentration of perchlorate ion is plotted in Fig. 15. As the concentration of perchlorate ions varies, two Nernstian linear ranges are observed: The change occurs at a concentration close to the concentration of nitrate ion in the sensor (over-Nernstian response). This can be explained based on ion exchange reaction given in the theory part (reaction I). When the concentration of perchlorate ion is lower than the concentration of nitrate ion in the organic phase, the sensor is still responding to nitrate ions. This is clearly manifested by a linear range at lower concentration of perchlorate. Where as the linear range at higher concentration perchlorate is because of perchlorate sensor after all the nitrate ions in the organic phase are replaced by perchlorate ions. The over-Nernstian response is due to shifting of potential from nitrate sensor to perchlorate sensor, which can be characterized by their standard Galvani potential difference. This can be evidenced by the change in potential between these two linear ranges. The potential change between them was found to be 148 mV which is in a reasonable agreement with a change in potential between the standard electric potential difference of the nitrate ion ($\Delta\phi^0 = -252 \text{ mV}$) and the standard electric potential difference of the perchlorate ion ($\Delta\phi^0 = -92 \text{ mV}$) [160 mV].

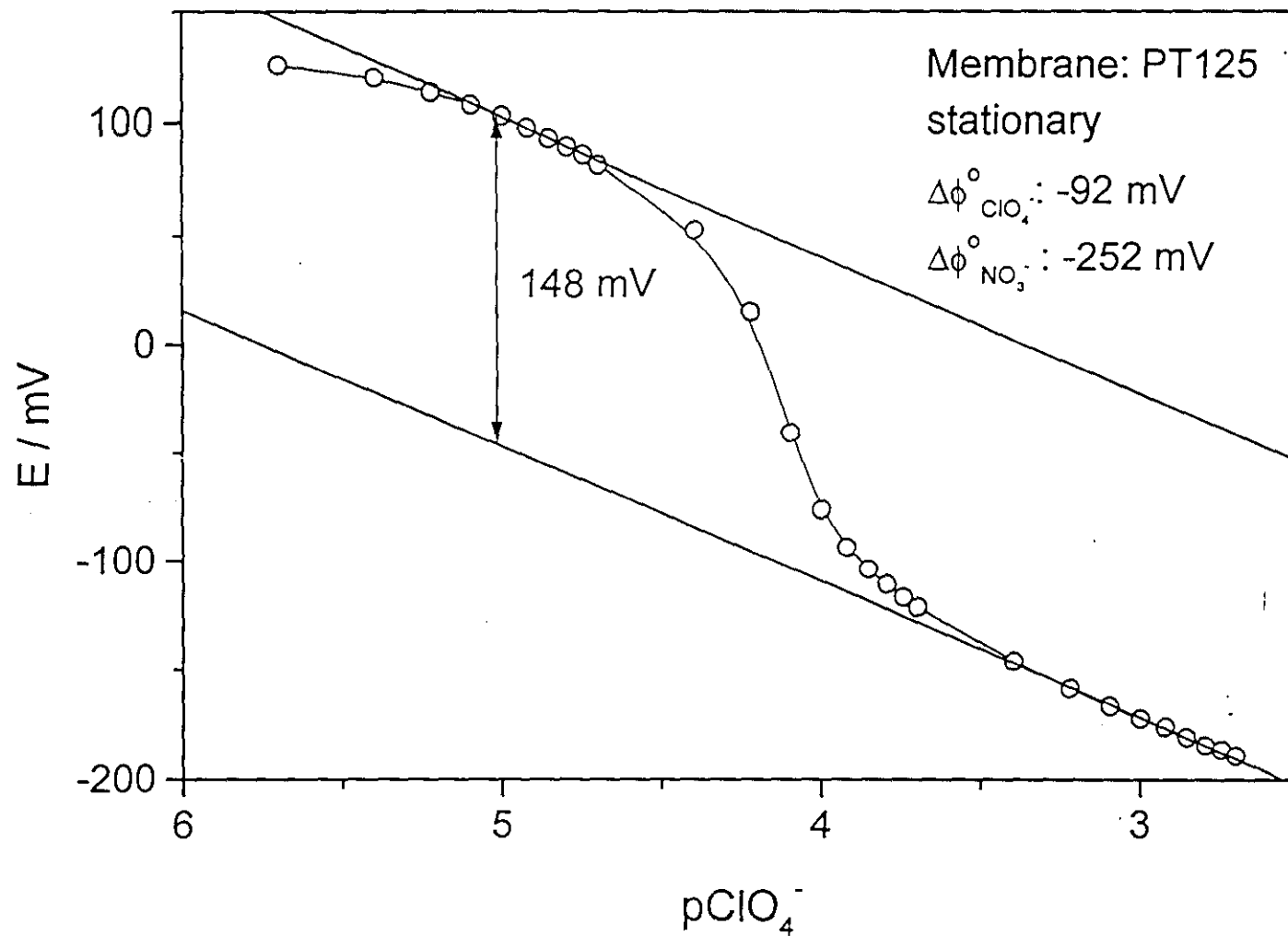


Fig. 15. Response of the nitrate sensor to perchlorate ions. Batch Injection of perchlorate ion into 50 ml of 0.1 M MgSO_4 .

In addition, the selectivity of the sensor based on the concept of ion exchange can also be studied. After the exchange equilibrium between interfering and primary ion, the concentration terms of them can be evaluated by assuming a certain x value to the interfering ion in the organic phase, and subtracting x from the initial concentrations of interfering and primary ions. These concentration terms are then inserted into eq. (5) which gives a quadratic equation. Finally the equation is solved and the roots values are inserted into the Nernst equation which estimates the response behavior of the sensor for each interfering ion.

In this regard, the calculated responses of the sensor to chloride, iodide and perchlorate ions are shown in Fig. 16. The response behaviors to iodide and perchlorate were similar even though the degree of interference of perchlorate ion is much higher than the iodide ion (estimated from the change in potential between the two linear ranges: I⁻, 53 mV and ClO₄⁻, 170 mV). But the response behavior of chloride is different from iodide and perchlorate. This stems from their hydrophilicity/hydrophobicity behaviors of these ions. The chloride ion ($\Delta G^0 = 31.8 \text{ kJ mol}^{-1}$) is more hydrophilic than the nitrate ion ($\Delta G^0 = 24.4 \text{ kJ mol}^{-1}$) whereas the iodide ion ($\Delta G^0 = 18.0 \text{ kJ mol}^{-1}$) and the perchlorate ion ($\Delta G^0 = 8.0 \text{ kJ mol}^{-1}$) ions are less hydrophilic than the nitrate ion. Besides, the calculated response of the sensor to these interfering ions was compared with the experimental results which were measured by FI technique.

In FI technique, the potential of the electrode is measured by injecting a series of different concentrations of the interfering ions. The technique is similar to the separate solution method where the electrode potential is separately measured for the interfering ion solution, and the primary ion solution without mixing one another.

The FI results to chloride and perchlorate are shown in Fig. 17. It is appeared that the calculate response of the sensor to these interfering ions is in a reasonable agreement with the experimental response of the sensor. In general, those ions which are hydrophobic strongly interfere with the nitrate sensor.

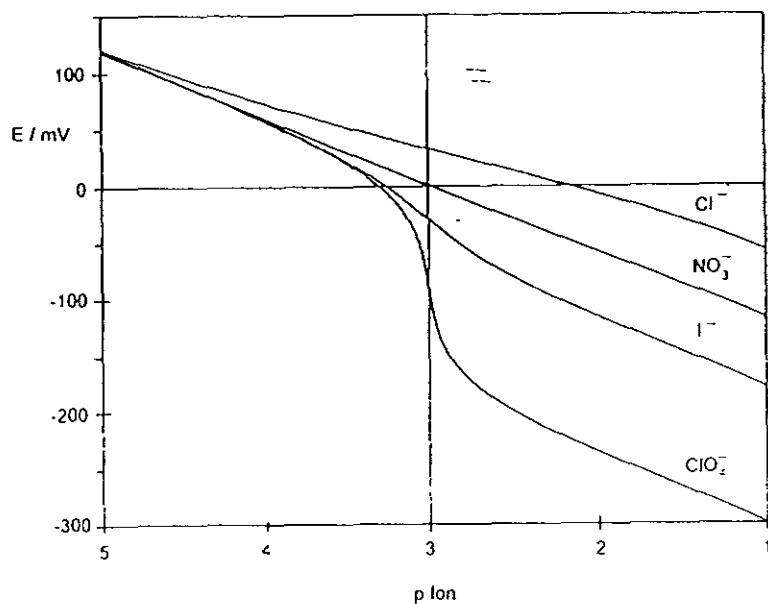


Fig. 16. Calculated response of a nitrate ISE to interfering ions Cl^- , I^- and ClO_4^-

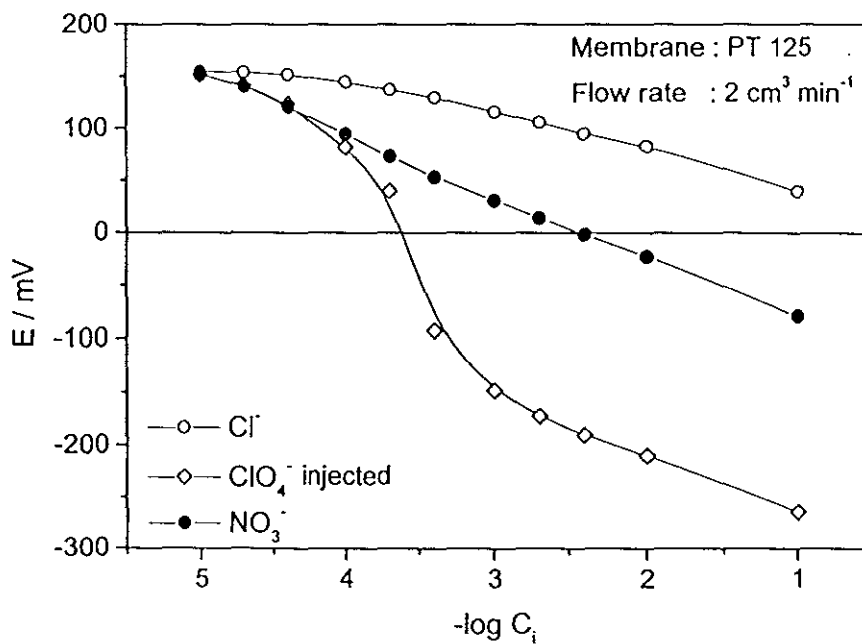


Fig. 17. Experimental response of nitrate sensor to the interfering ions, Cl^- and ClO_4^- under flow condition.

4.7. ANALYTICAL APPLICATION

4.7.1. POTENTIOMETRIC MEASUREMENT

To investigate the applicability of the sensor, tap water samples were taken. The amount of nitrate ion in the sample was found to be 4.20 mg l⁻¹ using direct measurement from the calibration graph of potentiometric sensor. But one of the drawbacks of the direct measurement is that it is not possible to match the composition of an unknown solution with the standard solution. One method of compensating for errors caused by activity coefficients is the standard addition method [39].

In this method, if C_x is the original concentration of the nitrate ion and C_s is the concentration of the standard solution being added, the concentration of the nitrate ion after n addition will be

$$(C_x)_n = \frac{VC_x + nC_sV_A}{V + nV_A} \quad (20)$$

where V is the original volume, and V_A is the volume of each addition. From the Nernst equation, the measured electrode potential for a nitrate sensor is

$$E_n = \text{const} - S \log (C_x)_n \quad (21)$$

where S is the slope. Rearranging and taking the antilog of eq. (21):

$$\text{antilog}\left(-\frac{E_n}{S}\right) = \text{constant} \left[\frac{VC_x + nC_sV_A}{V + nV_A} \right] \quad (22)$$

The left side of eq. (22) is plotted against $nC_sV_A / (V + nV_A)$, concentration of the standard solution. The x-intercept is then $-C_xV / (V + nV_A)$ from which the concentration of the nitrate ion can be evaluated (Fig. 18). Thus the amount of nitrate ion in tap water was found to be 3.22 mg l⁻¹.

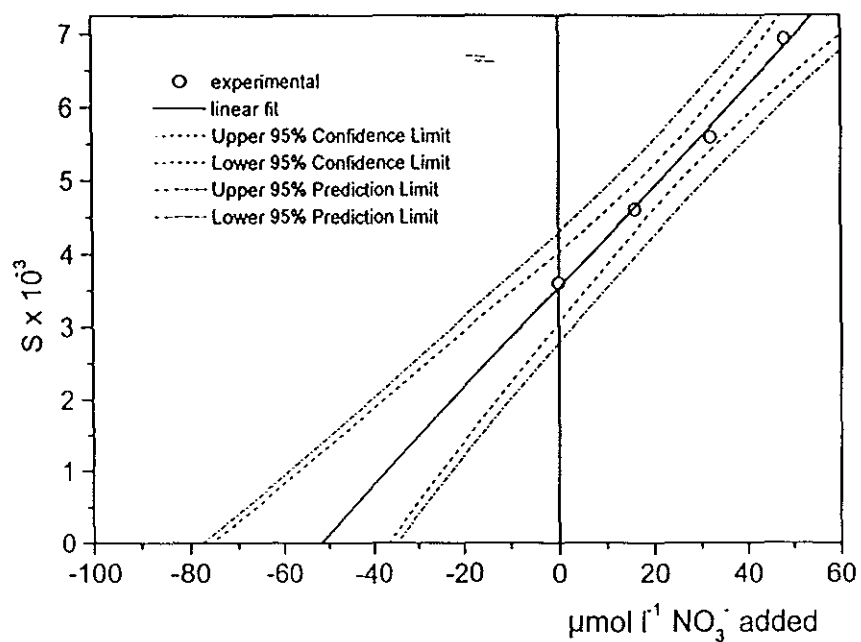


Fig. 18. Standard addition plot of potentiometric sensor.

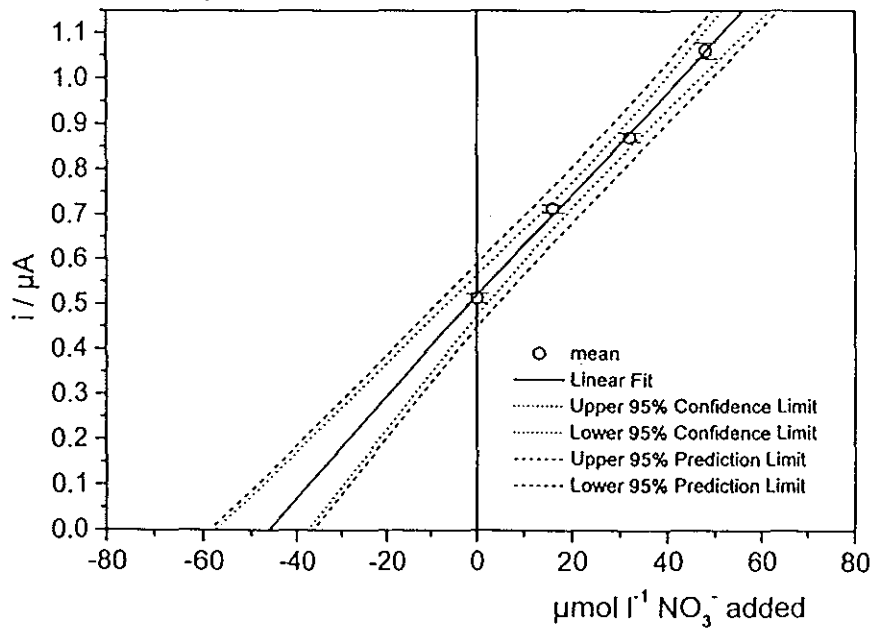


Fig. 19. Standard addition plot of amperometric sensor

4.7.2. AMPEROMETRIC MEASUREMENT

The standard addition plot of the amperometric sensor is shown in Fig. 19 from which the amount of nitrate ion in the same sample was found to be 2.91 mg l^{-1} . As seen from the standard addition graph, the 95 % confidence limit between upper and lower limit of the sensor response is in the range between 2.5 and 4.5 mg l^{-1} . This range of nitrate amount is in a good agreement with the range of nitrate amount found using potentiometric sensor above (Fig. 18).

4.7.3. UV-DETECTOR MEASUREMENT

As an independent method, without using the sensor, water samples were analyzed using UV-detector at 210 nm where the absorption of nitrate ion occurs (π - π^* transition). The recorder protocol of the calibration of the UV-detector with nitrate is shown in Fig. 20. Four injections of tap water sample (filtrated and untreated) were carried out and shown in Fig.20. As seen from the absorption peaks, the untreated sample is a bit lower than the filtrated sample, indicating the presence of physical interferences. To avoid this problem, the standard addition method were carried out. The recorder protocol and the standard addition graph are shown in Fig. 21 from which the amount of the nitrate ion was found to be 4.18 mg mol^{-1} .

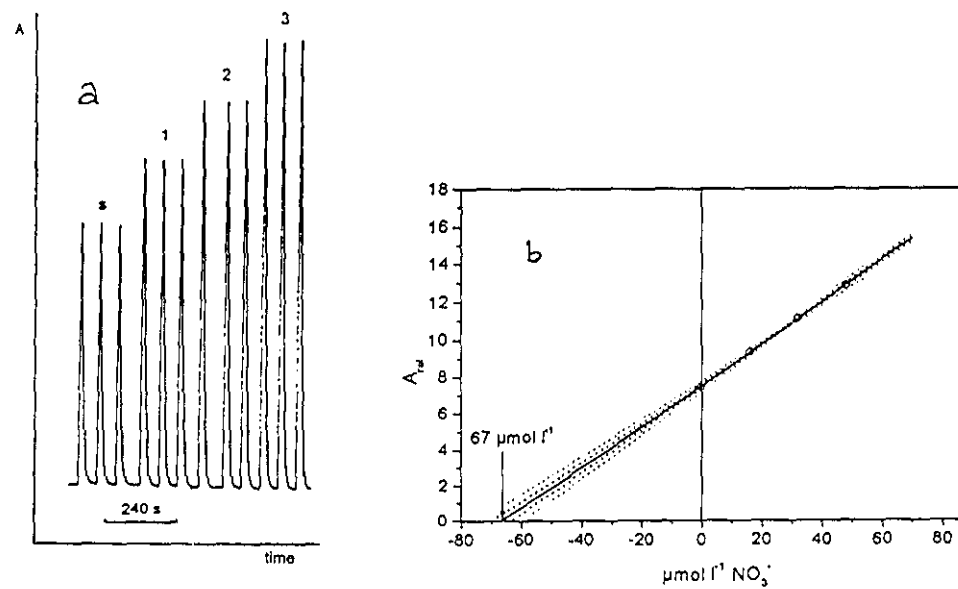


Fig. 21. a) Recorder protocol of the standard addition of the UV-detector with nitrate. S is without any addition. Numbers on top are standard concentrations of nitrate (1: 16; 2: 32 and 3: 48 μM)
 b) Standard addition plot.

6. REFERENCES

1. Harrison, R. M.; de Mora, S. J. *Introduction Chemistry for the Environmental Sciences*, 2nd ed., Cambridge Univ. Press: Cambridge, 1996, p. 181.
2. Plas-Qui, *McGraw-Hill Encyclopedia of Science and Technology*, 7th ed., Vol. 14, McGraw-Hill: New York, 1992, p. 95.
3. Skoog, D.A.; West, D.M. *Fundamentals of Analytical Chemistry*, 2nd ed., Hort, Rinehart and Winston: New York, 1969.
4. Rand, M. C.; Greenberg, A.E.; Taras, M. J. *Standard Methods for the Examination of Water and Waste Water*, 14th ed., APHA-AWWA-WPCF: Washington, 1976, p. 423.
5. Koryta, J. *Anal. Chim. Acta*, **1984**, *183*, 1.
6. Koryta, J. *Ann. Rev. Mater. Sci.*, **1986**, *16*, 13
7. Covington, A. K. *Ion-Selective Electrode Methodology*, Vol. I, CRC: Boca Raton, 1979.
8. Bailey, P.L. *Analysis with Ion-Selective Electrodes*, 2nd ed., Hyden: London, 1980.
9. Wilke, S.; Franzke, H.; Muller, H. *Anal. Chim. Acta*, **1992**, *268*, 285.
10. Koryta, J. *Electrochim. Acta*, **1979**, *24*, 293.
11. Sollner, K.; Sheam, G.M. *J. Am. Chem. Soc.*, **1964**, *86*, 1901.
12. Koryta, J., *Ion-Selective Electrode*, Cambridge Univ. Press: Cambridge, 1974, p. 4.
13. Sandblom, J.; Eisenman, G.; Walker, J. L. *J. Phys. Chem.* **1967**, *71*, 3862.
14. Srinivason, K.; Rechnitz, G. A. *Anal. Chem.*, **1969**, *41*, 1203.
15. Cunningham, L.; Freiser, H. *Anal. Chim. Acta.*, **1981**, *132*, 43.
16. Midgley, D., *Anal. Chem.*, **1977**, *49*, 1211.
17. Kakiuchi, T.; Senda, M. *Bull. Chem. Soc. Jpn.*, **1984**, *57*, 1801.
18. Kakiuchi, T.; Senda, M. *Bull. Chem. Soc. Jpn.*, **1985**, *58*, 1636.
19. Koryta, J. *Electrochim. Acta.*, **1984**, *29*, 445.
20. Hundhammer, B.; Solomon, T.; Alemayehu, B. *J. Electroanal. Chem.*, **1982**, *135*, 301.

21. Samec, Z.; Marecek, K.; Homolka, D. *J. Electroanal. Chem.*, **1981**, *126*, 121.
22. Kazarinov, V. E. *The Interface Structure and Electrochemical Processes at the Boundary Between two Immiscible Liquids*, Springer-Verlag: Berlin, 1987, p. 78.
23. Mekuria Habteyohannes *M. Sc-Thesis*, Department of Chemistry, Addis Ababa Univ. 1993.
24. Alemayehu Asfaw *M.Sc-Thesis*, Department of Chemistry, Addis Ababa Univ. 1994.
25. Ross, J. W. *Science*, **1964**, *156*, 1378.
26. Hundhammer, B.; Dhawan, S. K.; Bekele, A.; Seidlitz, H. J. *J. Electroanal. Chem.*, **1987**, *217*, 253.
27. Yamada, J.; Matsuda, H. *J. Electroanal. Chem.*, **1973**, *44*, 189.
28. Ruzicka, J.; Hansen, E. H. *Anal. Chim. Acta* **1973**, *78*, 145; *Flow Injection Analysis*, Wiley, New York, 2nd ed. 1988.
29. Hundhammer, B.; Wilke, S. *J. Electroanal. Chem.*, **1989**, *266*, 133.
30. Mulat Abegaz *M. Sc-Thesis*, Department of Chemistry, Addis Ababa Univ. 1990.
31. Hundhammer, B.; Solomon, T.; Zerihun, T.; Abegaz, M.; Bekele, A.; Graichen, K. *J. Electroanal. Chem.*, **1994**, *371*, 1.
32. Gunasingham, H.; Fleet, B. *Anal. Chem.*, **1983**, *55*, 1409.
33. Carslaw, H.; Jaeger, J. C. *Conduction of Heat in Solids*, Clarendon press: Oxford, 1959.
34. Adams, R. N. *Electrochemistry at Solid Electrodes*, Marcel Dekker: New York, 1969, p.70.
35. Burgess, C.; Knowles, A. *Standard in Absorption Spectrometry*, UV Spectrometry Group, Chapman and Hall: London, 1981, p. 3.
36. Ruff, J. K.; Schlientz, W. J. *Inorganic Syntheses*, **1974**, *15*, 84.
37. Wilke, S. *J. Electroanal. Chem.*, **1991**, *301*, 67.
38. Analytical Methods Committee, *Analyst*, **1987**, *112*, 199.
39. West, C. D. *Essentials of Quantitative Analysis*, McGraw-Hill: New York, 1987, p. 76.

DECLARATION

I, the undersigned, declare that this thesis is my original work and has not been presented for any degree in any other University and that all sources of material used for the thesis have been duly acknowledged.

Name: Solomon Mehretie

Signature: Solteh

This thesis has been submitted for examination with my approval as University Advisor.

Name: Dr. Bernd Hundhammer

Signature: Bernd Hundhammer

Date and place of Submission:

Department of Chemistry

Addis Ababa University

June, 1999

